ELSEVIER

Ceramics International 33 (2007) 895–900

CERAMICS
INTERNATIONAL

www.elsevier.com/locate/ceramint

Phase relation and microwave dielectric properties of $x\mathrm{CaTiO_3}$–$(1 - x)\mathrm{TiO_2}$–$3\mathrm{ZnTiO_3}$ multiphase ceramics

Fei Zhao, Zhenxing Yue *, Yongzhao Lin, Zhilun Gui, Longtu Li

State Key Laboratory of New Ceramics and Fine Processing, Department of Materials Science and Engineering,
Tsinghua University, Beijing 100084, PR China

Received 28 October 2005; received in revised form 28 November 2005; accepted 12 January 2006

Abstract

Microwave dielectric ceramics of $x\mathrm{CaTiO_3}$–$(1 - x)\mathrm{TiO_2}$–$3\mathrm{ZnTiO_3}$ (x = 0.05–1.00) were prepared by the solid-state reaction method. The phase relations were investigated using X-ray powder diffraction. In all the studied range, the sintered ceramic was multiphase, which was also verified by scanning electron microscopy (SEM) observation, as well as the energy-dispersive X-ray spectroscopy (EDX) analysis. With the increase of x from 0.05 to 0.25, the amount of rutile phase decreases due to the formation of new $Ca_2Zn_4Ti_{16}O_{38}$ polytitanates. And with x increasing from 0.25 to 1.00, rutile phase disappears while $CaTiO_3$ phase increases, accompanying with a slight decrease of $Ca_2Zn_4Ti_{16}O_{38}$. Thus, it is considered that the preferential chemical reaction in the system enhanced the formation of the $Ca_2Zn_4Ti_6O_{38}$ compound, $CaTiO_3$ and rutile phases in the ceramics. Moreover, the microwave dielectric properties of the ceramics were investigated. The simulated dielectric properties of the ceramics were also calculated based on the empirical model. The simulated results and the experimental ones have similar trends, which show that the change of microwave dielectric properties is related to the change of the phase composition in the multiphase ceramics.

Keywords: C. Dielectric properties; Ceramics; X-ray diffraction

1. Introduction

The development of microwave communication technology has been promoted by microwave dielectric ceramics. A large number of ceramic dielectric materials have been developed [1] over the years. The accustomed scheme for developing new dielectric materials has focused on considering new single-phase solid solutions having high Q or high dielectric constant. However, it is interesting to note that some compounds often formed multiphase mixtures, rather than single-phase solid solutions. In fact, composition route is usually used to adjust the temperature coefficient of resonant frequency (TCF) in dielectric composition study. The formation of multiphase made the dielectric properties optimization more complicated. Recently, the development of low-temperature cofired ceramic (LTCC) processing encouraged the investigation of some low sintering temperatures compounds [2–4], in which zinc titanates and their modified systems are of important kinds due to the relatively low sintering temperatures and promising dielectric properties. The dielectric properties of pure $ZnTiO_3$ ceramics were investigated by Sugiura and Ikeda [5]. Haga et al. [6] reported the dielectric properties of $ZnTiO_3$–TiO_2 systems and identified the zero temperature coefficients of dielectric constant. Kim et al. [4] investigated the low-temperature sintering $ZnTiO_3$–TiO_2 systems using B_2O_3. They also investigated the microstructure and microwave dielectric properties of alkaline earth modified zinc titanates [7,8]. It revealed that doping temperature compensating compounds such as TiO_2 or $CaTiO_3$ into zinc titanates always induces complicated phase compositions [4,6–8]. Therefore, it was quite indispensable to study the phase relations and composition variations in TiO_2 or $CaTiO_3$-doped zinc titanate system. The prior works [4,6,7] only focused on either $ZnTiO_3$–TiO_2 or $ZnTiO_3$–$CaTiO_3$ systems in the pseudo-ternary CaO–ZnO–TiO_2 phase, as shown in Fig. 1 (open and solid circles, and here, $ZnTiO_3$ abbreviated as 'ZT', TiO_2 abbreviated as 'R' and $CaTiO_3$ abbreviated as 'CT'). Furthermore, the phase relations and the relationship of phase compositions and dielectric properties in the pseudo-ternary CaO–ZnO–TiO_2 phase have not been satisfactory.

---

* Corresponding author. Tel.: +86 10 62784579; fax: +86 10 62771160.
E-mail address: yuezhx@tsinghua.edu.cn (Z. Yue).

0272-8842/$32.00
doi:10.1016/j.ceramint.2006.01.015

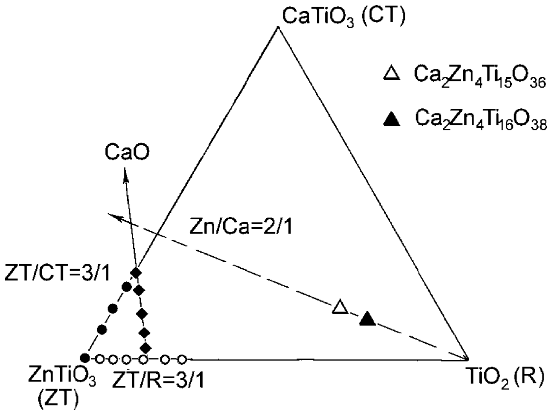

Fig. 1. CaO–ZnO–TiO_2 ternary system and the composition regions of previous works [4,7] and the present works in the system (open and solid circles for Ref. [4,7], respectively; solid diamond is the region of present works).

In this study, the $x$$CaTiO_3$–$(1 - x)$$TiO_2$–3$ZnTiO_3$ system was selected, as shown in Fig. 1 (solid diamonds). The phase relations, as well as the relationship between phase compositions and microwave dielectric properties of the multiphase ceramics were investigated. The difference between the present works and the previous reports [7] was also indicated and discussed.

2. Experimental procedure

Samples of $x$$CaTiO_3$–$(1 - x)$$TiO_2$–3$ZnTiO_3$ with $x = 0.05$–1.00 were synthesized from high-purity (more than 99.9%) powders of $CaCO_3$, ZnO and TiO_2 (anatase), using the conventional solid-state reaction method. The oxides and carbonate were weighed according to the desired molar ratio. The mixtures were ball-milled in a polyethylene jar for 4 h using zirconia balls in alcohol medium. The milled powders were dried and then calcined at 900 °C for 2 h. The calcined powders were remilled, dried, mixed with an appropriate amount of PVA (5 wt.%) as a binder and then screened by a 60 mesh. The screened powders were pressed into cylindrical disks of diameter 10 mm and height about 5 mm at a pressure of about 2000 kg/cm^2. These pellets were preheated at 550 °C for 3 h to expel the binder and then sintered at temperatures from 1050 to 1200 °C for 4 h in air.

The crystalline phase of the sintered samples were determined by X-ray diffraction (XRD), using Cu Kα radiation. The microstructures of samples were observed by scanning electron microscopy (SEM). The chemical compositions of the phases formed were elucidated by energy-dispersive X-ray spectroscopy (EDX). An HP8720ES network analyzer was employed in the measurement of microwave dielectric properties. The dielectric constant was measured at microwave frequencies in room temperature using the Hakki–Coleman [9] dielectric resonator method. The quality factor was measured by transmission cavity method [10]. The temperature coefficients of resonant frequencies (TCF) were measured in the temperature range of 20–80 °C. The TCF value can be calculated by the following relationship:

$$\mathrm{TCF} = \frac{f_2 - f_1}{f_1(T_2 - T_1)} \tag{1}$$

where f_1 and f_2 represent the resonant frequencies at T_1 and T_2, respectively.

3. Results and discussions

XRD analysis of wide range ($2\theta = 10$–80°) was performed on different $x$$CaTiO_3$–$(1 - x)$$TiO_2$–3$ZnTiO_3$ powders and ceramics sintered at different temperatures. However, the diffraction peaks higher than $2\theta = 40°$ were hard to distinguish from each other, due to low intensities or overlap of peaks. Thus in the present paper, only the characteristic patterns in the 2θ range 10–38° was carefully indexed. Fig. 2 shows the $x$$CaTiO_3$–$(1 - x)$$TiO_2$–3$ZnTiO_3$ ($x = 0.25$) powders calcined from 900 to 1050 °C for 2 h. For the powders calcined at 900 °C, six phases were obtained including $Zn_2Ti_3O_8$, $ZnTiO_3$, Zn_2TiO_4, $CaTiO_3$, anatase and rutile phases. For the powders calcined at 950 °C, the peaks of $Zn_2Ti_3O_8$, $ZnTiO_3$ and anatase phases disappeared, while the major peak of rutile phase increased. It was understood that most of the anatase phase transformed into rutile phase with increasing calcined temperature from 900 to 950 °C. Moreover, a new phase formed, which was identified as $Ca_2Zn_4Ti_{16}O_{38}$, rather than $Ca_2Zn_4Ti_{15}O_{36}$ reported by Kim et al. [7]. According to the earlier reports [11,12], there are two compounds in CaO–ZnO–TiO_2 ternary phase diagram, which are $Ca_2Zn_4Ti_{15}O_{36}$ (empty triangle) and $Ca_2Zn_4Ti_{16}O_{38}$ (filled

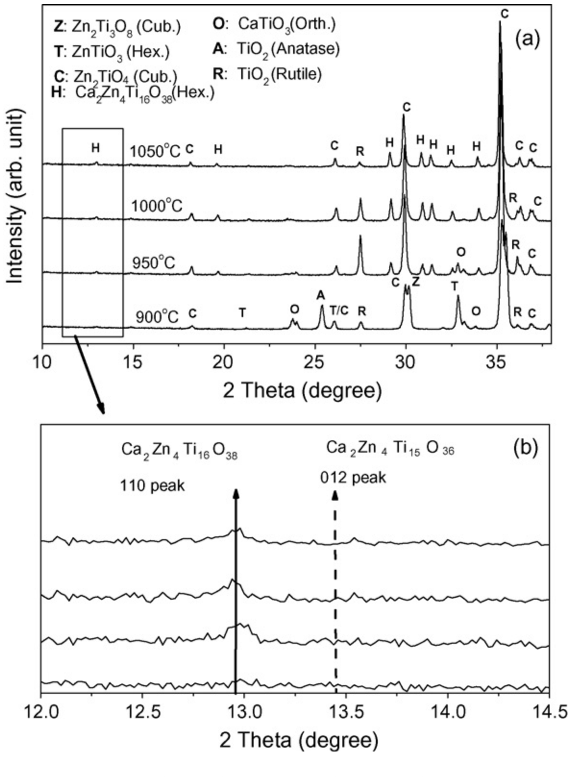

Fig. 2. XRD patterns of $x$$CaTiO_3$–$(1 - x)$$TiO_2$–3$ZnTiO_3$ powders ($x = 0.25$) calcined at temperature range 900–1050 °C for 2 h.

triangle, Fig. 1). It can be seen that they are similar compounds. In addition, the XRD patterns of these two compounds are similar (JCPDS files No. 34-0055 and 85-1102). However, these two compounds can still be distinguished by the difference in reflection lines around $2\theta \sim 13^\circ$. The 2θ of reflection line 1 1 0 ($2\theta = 12.965^\circ$) in $Ca_2Zn_4Ti_{16}O_{38}$ pattern is a bit lower than that of the reflection line 0 1 2 ($2\theta = 13.446^\circ$) in $Ca_2Zn_4Ti_{15}O_{36}$ pattern. Therefore, it is feasible to distinguish between $Ca_2Zn_4Ti_{16}O_{38}$ and $Ca_2Zn_4Ti_{15}O_{36}$, as shown in Fig. 2b. With further increase of calcined temperature from 950 to 1050 °C, the peaks of rutile and $CaTiO_3$ phases decreased or disappeared, accompanying with a slight increase of the peaks of $Ca_2Zn_4Ti_{16}O_{38}$. There existed only three phases for the powder calcined at 1050 °C, which were Zn_2TiO_4, $Ca_2Zn_4Ti_{16}O_{38}$ and rutile phases. It can be seen in Fig. 2a that both hexagonal $ZnTiO_3$ phase and cubic $Zn_2Ti_3O_8$ phase decomposed partially at 900 °C and completely into cubic Zn_2TiO_4 and rutile phases at 950 °C, which are in agreement with the earlier reports [4]. The XRD patterns also reveal that the formation of $Ca_2Zn_4Ti_{16}O_{38}$ started at about 950 °C, which was not mentioned in previous literatures. It has been reported that $CaTiO_3$ completely formed at about 920 °C [13]. Thus, the Ca^{2+}-containing reactant which formed $Ca_2Zn_4Ti_{16}O_{38}$ is $CaTiO_3$, rather than $CaCO_3$ or CaO. Accordingly, the reactions of xCaTiO$_3$–$(1-x)$TiO$_2$–3ZnTiO$_3$ powders can be expressed as follows:

$$ZnO + TiO_2(\text{anatase}) \xrightarrow{\leq 900\,^\circ C} ZnTiO_3 \tag{2}$$

$$4ZnTiO_3 \xrightarrow{\sim 900\,^\circ C} Zn_2Ti_3O_8 + Zn_2TiO_4 \tag{3}$$

$$Zn_2Ti_3O_8 \xrightarrow{900\text{–}950\,^\circ C} Zn_2TiO_4 + 2TiO_2\ (\text{rutile}) \tag{4}$$

$$CaCO_3 + TiO_2(\text{anatase}) \xrightarrow{\leq 900\,^\circ C} CaTiO_3 + CO_2\uparrow \tag{5}$$

$$2CaTiO_3 + 2Zn_2TiO_4 + 12TiO_2(\text{rutile}) \xrightarrow{\geq 950\,^\circ C} Ca_2Zn_4Ti_{16}O_{38} \tag{6}$$

Fig. 3 shows the XRD patterns of xCaTiO$_3$–$(1-x)$TiO$_2$–3ZnTiO$_3$ ceramics sintered at 1150 °C for 4 h. The sintered ceramic was multiphase, as marked in Fig. 3. The peaks of α-Zn_2TiO_4, $Ca_2Zn_4Ti_{16}O_{38}$, $CaTiO_3$ and rutile phases were observed in different compositions. For the samples of $x = 0.05$ Ca^{2+} contents, no $CaTiO_3$ phases were observed and α-Zn_2TiO_4 and rutile were the major phases. With Ca^{2+} contents increase, the peaks of rutile became weak and those representing the compound of $Ca_2Zn_4Ti_{16}O_{38}$ grew stronger. It was understood that the increase of Ca^{2+} content enhanced the formation of $Ca_2Zn_4Ti_{16}O_{38}$, which reduced the rutile phase effectively. When $x = 0.50$, $CaTiO_3$ phase was observed and rutile phase disappeared. It was because that the increase of Ca^{2+} ions content increased the amount of $CaTiO_3$ phase and the enough $CaTiO_3$ phase eliminated the rutile phase by the formation of more $Ca_2Zn_4Ti_{16}O_{38}$. When $x = 1.00$, more $CaTiO_3$ phase formed. However, due to the lack of rutile phase, the amount of $Ca_2Zn_4Ti_{16}O_{38}$ decreased and more residual $CaTiO_3$ phase was observed. The formation of $Ca_2Zn_4Ti_6O_{38}$ related to the stability of $CaTiO_3$, TiO_2 and $ZnTiO_3$ in the system and the preferential chemical reaction in the system enhanced the formation of the $Ca_2Zn_4Ti_6O_{38}$ compound.

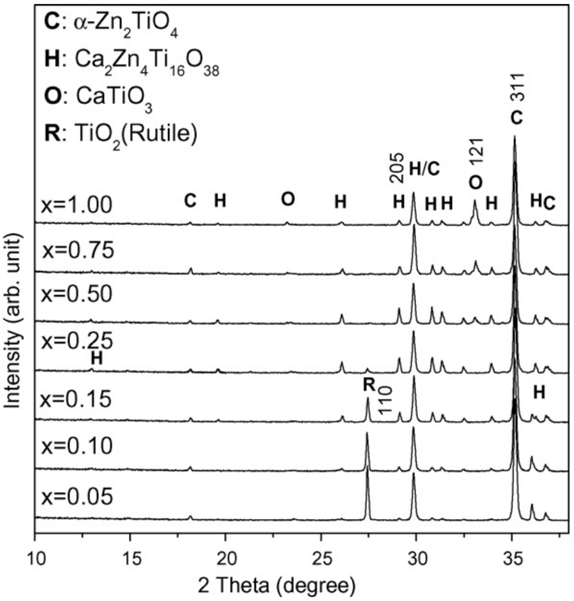

Fig. 3. XRD patterns of xCaTiO$_3$–$(1-x)$TiO$_2$–3ZnTiO$_3$ powders synthesized at 1150 °C for 4 h as a function of x.

In order to illuminate the amount of different phases more effectively, major peaks of the different phases were selected to calculate the weight fraction of each phase by Matrix-Flushing method ('value-K' method) [14]. The results were transformed into molar fraction and plotted as a function of Ca^{2+} content (x), as shown in Fig. 4. It can be seen that the major phase of the mixtures is α-Zn_2TiO_4 phase. The amount of $Ca_2Zn_4Ti_{16}O_{38}$ phase increases with decrease of rutile phase, while it decreases with increase of $CaTiO_3$ phase, which is in agreement with the above analysis of the reaction sequence. Moreover, it would be interesting to know whether the X-ray determined phase fraction ratios are in agreement with the overall compositions. Therefore, a list of calculated compositions for the mixtures is given in Table 1. It can be seen that the X-ray determined phase

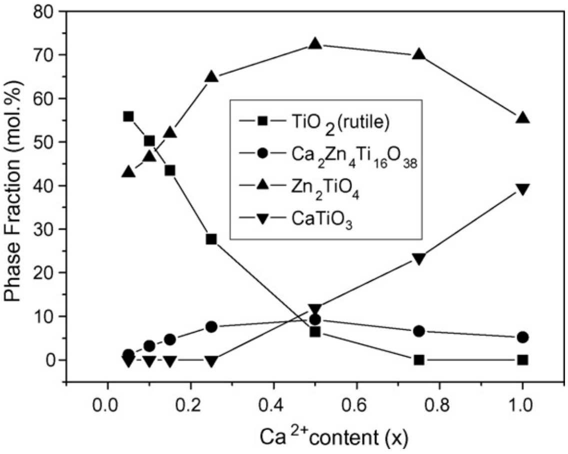

Fig. 4. The variation of phase fraction (mol.%) as a function of x.

Table 1
Calculated compositions for the multiphase system

x	TiO_2 (rutile)	$Ca_2Zn_4Ti_{16}O_{38}$	α-Zn_2TiO_4	$CaTiO_3$
0.05	86/145	1/145	58/145	0
0.10	108/195	3/195	84/195	0
0.15	58/115	3/115	54/115	0
0.25	6/17	1/17	10/17	0
0.50	4/53	5/53	38/53	6/53
0.75	0	7/87	58/87	22/87
1.00	0	1/17	10/17	6/17

fraction ratios are in agreement the overall compositions. Thus, the discussions above are reasonable and reliable.

The microstructures of xCaTiO$_3$–(1 − x)TiO$_2$–3ZnTiO$_3$ ceramics were observed using scanning electron microscopy. Fig. 5 illustrates the typical SEM images of sintered samples with various compounds sintered at 1150 °C. Fig. 5a and b shows the second electron images of $x = 0.75$ (surface) and $x = 0.25$ (fractured section). Fig. 5c and d shows the backscattered electron images of their counterparts. The second electron images show that the well-densified microstructures were obtained and almost no porosities were observed in the sintered samples. The backscattered electron images show clearly the distributions of different phases. Phases of α-Zn_2TiO_4, $Ca_2Zn_4Ti_{16}O_{38}$, $CaTiO_3$ and rutile were identified according to the results of EDX analysis. Except for a few abnormal grains, all phases have average grain sizes of 3–6 μm with random distributions. The abnormal grains have a larger grain size of 10–15 μm, which also distributes randomly. Due to the small grains and random distributions of each phase, the theoretical value of the multiphase ceramics can be calculated and the results are creditable, which will be discussed later.

As part of the multiphase investigations, the dielectric properties of xCaTiO$_3$–(1 − x)TiO$_2$–3ZnTiO$_3$ ceramics at microwave frequencies were measured on the sintered ceramics. The variations of dielectric constant, $Q \times f$ value and TCF value with x for xCaTiO$_3$–(1 − x)TiO$_2$–3ZnTiO$_3$ ceramics are shown in Fig. 6 (full symbols). With x increasing from 0.05 to 0.25, $Q \times f$ value increases from 19,000 to 23,500 GHz, while dielectric constant decreases from 36.4 to 32.0, and TCF value from +68 to +33 ppm/°C. With x increasing from 0.25 to 1.00, $Q \times f$ value decreases from 21,500 to 11,000 GHz, while dielectric constant increases from 32.0 to 50.9, and TCF value from +34 to +240 ppm/°C. The variations of microwave dielectric properties are considered to be related to the change of different phase compositions in the mixtures. To prove this, the well-known general empirical model was employed in the multiphase ceramics. The simulated dielectric constant and TCF of the samples were obtained by the following equations [15,16]:

$$\varepsilon_r^\alpha = \sum X_i \varepsilon_{ri}^\alpha \tag{7}$$

$$\mathrm{TCF} = \sum X_i \mathrm{TCE}_i \tag{8}$$

where X_i, ε_{ri}, and TCF$_i$ are the volume fraction, dielectric constant and TCF of the ith phase (i = 1, 2, 3, 4), respectively, and α is a constant. The value of α determines the type of

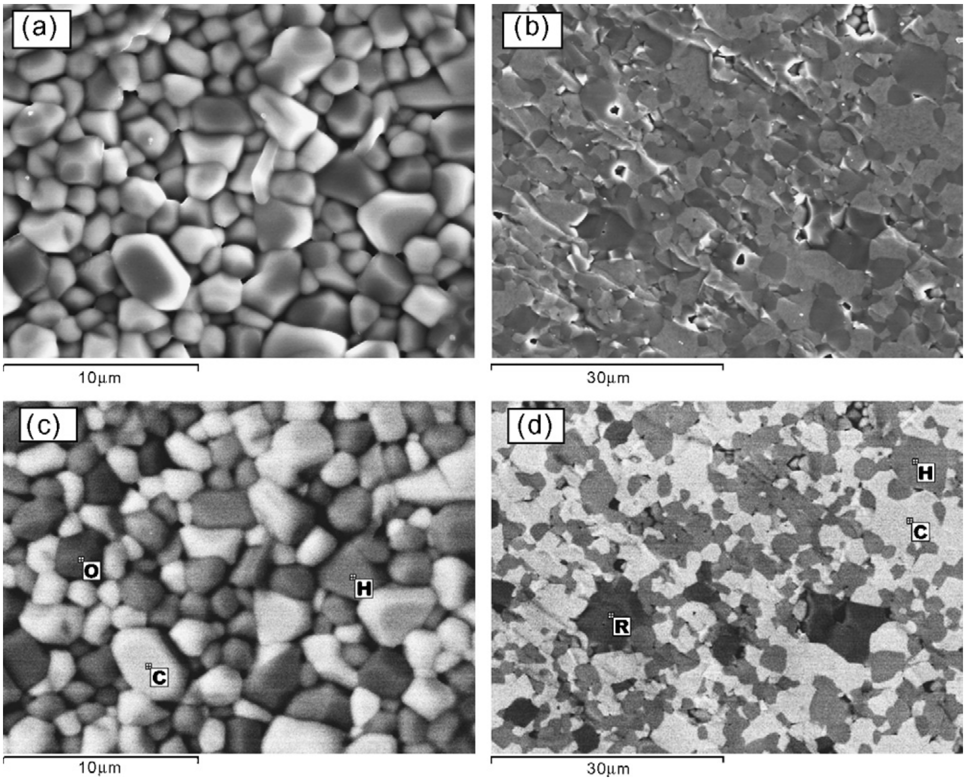

Fig. 5. SEM images of xCaTiO$_3$–(1 − x)TiO$_2$–3ZnTiO$_3$ ceramics: second electron images of (a) surface of $x = 0.75$ and (b) fractured section of $x = 0.25$; backscattered electron images of (c) surface of $x = 0.75$ and (d) fractured section of $x = 0.25$.

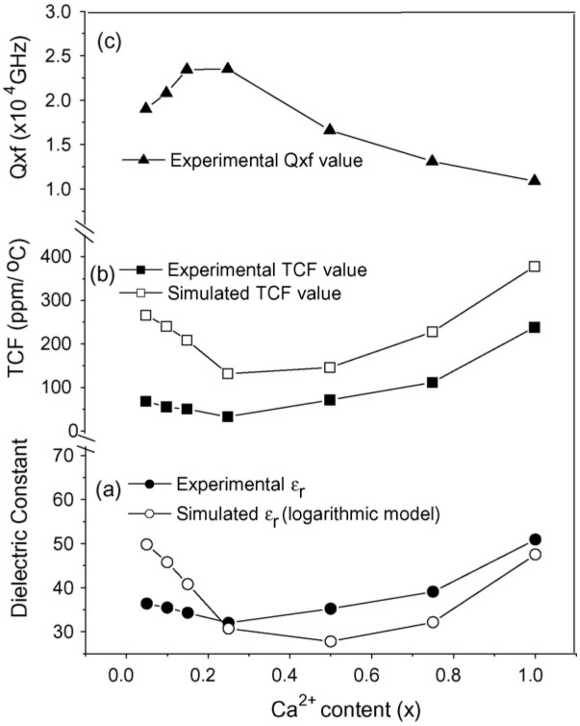

Fig. 6. The variations of experimental (full symbols) and calculated (open symbols) microwave dielectric properties with *x* for xCaTiO$_3$–$(1-x)$TiO$_2$–3ZnTiO$_3$ ceramics.

mixing rule: $\alpha = -1$, 1 and 0 represents serial, parallel and logarithmic mixing model, respectively. The volume fraction was calculated from the weight fraction of each phase, the dielectric constant and the TCF of each phase were obtained from the refs. [17–19] and our previous works. Fig. 6a (open symbols) shows the results of dielectric constant simulated using logarithmic models. The result of TCF calculated using Eq. (8) is shown in Fig. 6b (open symbols). The trends of simulated results are in agreement with that of experimental ones to a certain extent, whereas the values of simulated results are of some difference. The difference between the calculated values and the experimental ones may be due to these following reasons: firstly, the uncertainty of calculated volume fraction is unavoidable; secondly, the distribution of different phases was not perfect uniformity; finally, the microwave dielectric properties of each phase may be different in the mixture comparing with those in the monophase ceramics, which may be owing to the diffusion of different atoms or the formation of solid solution phases in the mixture. Therefore, although the microwave dielectric properties of the multiphase ceramics are mainly decided by the phase compositions of ceramics, the effects of diffusion or the formation of solid solution phases must be considered during the optimizations of multiphase materials.

4. Conclusions

The phase relations, microstructure and microwave dielectric properties of xCaTiO$_3$–$(1-x)$TiO$_2$–3ZnTiO$_3$ ceramics were investigated as a function of Ca^{2+} content (x). With the increase of Ca^{2+} content (x), the phase compositions changed. The preferential chemical reaction in the system enhanced the formation of the $Ca_2Zn_4Ti_6O_{38}$ compound. With x increasing from 0.05 to 0.25, new $Ca_2Zn_4Ti_{16}O_{38}$ polytitanates phase formed and the residual rutile phase decreases. With x increasing from 0.25 to 1.00, $CaTiO_3$ phase increases while $Ca_2Zn_4Ti_{16}O_{38}$ slightly decreases and rutile phase disappears. The variations of both experimental and simulated microwave dielectric properties show ‘‘v’’-shape trends, whereas there is obvious difference in the simulated values and the experimental ones. The results show that the microwave dielectric properties of the multiphase ceramics are not only related to the phase composition in the mixtures but also to the effects of diffuseness or the formation of solid solution phases.

Acknowledgements

This work has been financially supported by the National High-Tech Development Project of China (Grant No. 2001AA325100), the National Major Fundamental Research Project (Grant No. 2002CB613307), and SRFDP (No. 20040003003).

References

[1] W. Wersing, Microwave ceramics for resonators and filters, Curr. Opin. Solid State Mater. Sci. 1 (1996) 715–731.
[2] C.L. Huang, R.J. Lin, J.J. Wang, Effect of B_2O_3 additives on sintering and microwave dielectric behaviors of CuO-doped $ZnNb_2O_6$ ceramics, Jpn. J. Appl. Phys. 41 (2002) 758–762.
[3] S.H. Wee, D.W. Kim, S.I. Yoo, Microwave dielectric properties of low-fired $ZnNb_2O_6$ ceramics with $BiVO_4$ addition, J. Am. Ceram. Soc. 87 (2004) 871–874.
[4] H.T. Kim, S.H. Kim, S. Nahm, J.D. Byun, Low-temperature sintering and microwave dielectric properties of zinc metatitanate-rutile mixtures using boron, J. Am. Ceram. Soc. 82 (1999) 3043–3148.
[5] M. Sugiura, K. Ikeda, Studies on the dielectrics of the TiO_2-ZnO system, J. Jpn. Ceram. Assoc. 55 (1947) 62–66.
[6] K. Haga, T. Ishii, J. Mashiyama, T. Ikeda, Dielectric properties of two-phase mixture ceramics composed of rutile and its compounds, Jpn. J. Appl. Phys. 31 (1992) 3156–3159.
[7] H.T. Kim, J.D. Byun, Y. Kim, Microstructure and microwave dielectric properties of modified zinc titanates (I), Mater. Res. Bull. 33 (1998) 963–973.
[8] H.T. Kim, J.D. Byun, Y. Kim, Microstructure and microwave dielectric properties of modified zinc titanates (II), Mater. Res. Bull. 33 (1998) 975–986.
[9] B.W. Hakki, P.D. Coleman, A dielectric resonator method of measuring inductive in the millimeter range, IRE Trans. Microwave Theory Tech. MMT-8 (1960) 402–410.
[10] W.E. Courtney, Analysis and evaluation of a method of measuring the complex permittivity and permeability of microwave insulators, IEEE Trans. Microwave Theory Tech. MMT-18 (1970) 476–485.
[11] S.F. Bartram, W.M. Foss, Compound formation and crystal structure in the system ZnO–TiO_2, J. Am. Ceram. Soc. 64 (1981) 80–84.
[12] B.M. Gatehouse, I.E. Grey, The crystal structure of $Ca_2Zn_4Ti_{16}O_{38}$, J. Solid State Chem. 46 (1983) 151–155.
[13] I.R. Evans, J.A.K. Howard, T. Sreckovic, M.M. Ristic, Variable temperature in situ X-ray diffraction study of mechanically activated

synthesis of calcium titanate, $CaTiO_3$, Mater. Res. Bull. 38 (2003) 1203–1213.

[14] F.H. Chung, Quantitative interpretation of X-ray diffraction patterns of mixtures. I. Matrix-flushing method for quantitative multicomponent analysis, J. Appl. Cryst. 7 (1974) 519–525.

[15] W.D. Kingery, Introduction to Ceramics, second ed., Wiley, New York, 1976, p. 947.

[16] A.E. Paladino, Temperature-compensated $MgTi_2O_5$–TiO_2 dielectrics, J. Am. Ceram. Soc. 54 (1971) 168–169.

[17] P.L. Wise, I.M. Reaney, W.E. Lee, T.J. Price, D.M. Iddles, D.S. Cannell, Structure-microwave property relations in $(Sr_xCa_{1-x})_{n+1}Ti_nO_{3n+1}$, J. Eur. Ceram. Soc. 21 (2001) 1723–1726.

[18] A. Templeton, X. Wang, S.J. Penn, S.J. Webb, L.F. Cohen, N. McN Alford, Microwave dielectric loss of titanium oxide, J. Am. Ceram. Soc. 83 (2000) 95–100.

[19] A. Golovchansky, H.T. Kim, Y. Kim, Zinc titanates dielectric ceramics prepared by sol–gel process, J. Kor. Phys. Soc. 32 (1998) S1167–S1169.